CSCE Annual Conference

Growing with youth – Croître avec les jeunes

Laval (Greater Montreal)

June 12 - 15, 2019

EFFECTS OF STAGGERING ON THE SPLICE STRENGTH OF BUNDLED GFRP BARS IN CONCRETE

Asadian, A.[1,2]; Eslami, A. [1,3]; Farghaly, S. A. [1,4]; Benmokrane, B. [1,5]
[1] Université de Sherbrooke, Canada
[2] alireza.asadian@usherbrooke.ca
[3] a.eslami@usherbrooke.ca
[4] ahmed.sabry.abd.farghaly@usherbrooke.ca
[5] brahim.benmokrane@usherbrooke.ca

- **Abstract:** Although bundling of reinforcing bars is sometimes unavoidable in field applications, the scarcity of design provisions in the international design guidelines has limited the application of bundled glass fiber-reinforced polymer (GFRP) bars in reinforced concrete members. This is mainly attributed to the lack of experimental data on the lap splicing of bundled GFRP bars. Therefore, a comprehensive research study has been undertaken at the University of Sherbrooke to fill the current knowledge gap and provide more information about the bond behavior of staggered and non-staggered bundled GFRP bars in concrete. The current study reports and discusses the results of seven full-scale beams with different staggering patterns (staggered and non-staggered) and number of bars in bundle (single, two- and three-bar bundles). All beams had a clear span of 5000 mm, a shear span of 1250 mm and a constant-moment span of 2500 mm. The gross cross-sectional dimensions of all specimens were 300×450 mm. The experimental results indicated that regardless of staggering pattern, splicing of two-bar bundles is a safe practice. It was also shown that splicing of three-bar bundles is a safe practice as long as all bars in a bundle are not spliced at the same section.

Keywords: Reinforced Concrete, lap splicing; bond strength; GFRP reinforcing bar, bundled bars; staggering effect.

1 INTRODUCTION

Glass fiber-reinforced polymer (GFRP) reinforcing bars are intrinsically corrosion resistant. They also possess large strength-to-weight ratios, low life-cycle maintenance costs, and outstanding electromagnetic transparency. These superior characteristics are the reasons why GFRPs are considered as a distinct alternative to steel bars where corrosion in reinforced concrete (RC) structures is the main concern, and high electromagnetic transparency is important.

Splicing of reinforcing bars is one of the main means of joining reinforcing bars with different length or size. Bundling is sometimes inevitable when design criteria require heavy reinforcement to avoid reinforcement congestion, to reduce the overall cross-sectional dimensions, and to facilitate the placement of reinforcing bars and consolidation of concrete. However, as per available design guidelines (Canadian Standards Association, 2012; ACI Committee 318, 2014), the splicing of bundled bars may require some considerations and the splices need to be staggered in field applications. Although staggering may lead to

reduction in reinforcement congestion, it can increase the complexity of detailing and impede reinforcement placement, thereby hampering the construction process.

Despite the benefits of using bundled GFRP bars in RC members, its application has been limited due to the paucity of design provisions in most of the international design guidelines such as JSCE-97 (Japan Society of Civil Engineers, 1997), CSA S06-14 (Canadian Standards Association, 2014) and ACI 440.1R-15 (ACI Committee 440, 2015). This scarcity is mainly attributed to the lack of experimental data on the lap splicing of bundled FRP bars. The available design recommendations are similar to those for steel reinforcing bars. However, the bond behavior of GFRP bars in concrete is to a great extent different than that of steel reinforcement due to their diverse mechanical and physical characteristics, such as lower modulus of elasticity and various surface treatments.

The behavior of spliced single GFRP bars to concrete has been extensively investigated in the past (Tighiouart et al., 1999; Aly et al., 2006b; Mosley et al., 2008; Harajli & Abouniaj, 2010; Choi et al., 2012; Esfahani et al., 2013; Pay et al., 2014; Zemour et al., 2018). Based on the obtained results, the influencing parameters on the bond strength of GFRP bars includes, but are not limited to, splice length, bar diameter, confinement, surface treatment, and concrete type and compressive strength. It should be noted that, all available experimental studies attended to FRP bars spliced in the same section.

While several research studies (Tighiouart et al., 1999; Aly et al., 2006b; Mosley et al., 2008; Harajli & Abouniaj, 2010; Choi et al., 2012; Esfahani et al., 2013; Pay et al., 2014; Zemour et al., 2018) referred to the behavior of splices of single bars, only Aly et al.(Aly et al., 2006a) studied the spliced bundled FRP bars. In their study, a total of nine full-scale beam-splice tests were performed to assess the effects of the number of bars in a bundle on the bond strength of sand-coated CFRP bars. Their results indicated that the development length of individual bars within a bundle might be equal to that of a single bar, increased by 60% and 100% for two-and three-bar bundles, respectively. This conclusion raised a question on the reliability of the current provisions stipulated in CSA S806-12(Canadian Standards Association, 2012). Nevertheless, the splice arrangement adopted by Aly et al. (Aly et al., 2006a) was not in accordance with the design recommendations of CSA S806-12, as all the bars were spliced in the same section. It is worth noting that, no other experimental studies on the bond strength of bundled FRP bars are available in the technical literature. Therefore, a comprehensive research study has been undertaken at the University of Sherbrooke to fill the current knowledge gap and to provide more information about the bond behavior of staggered and non-staggered bundled GFRP bars in concrete. Herein, a part of this research program is reported and discussed.

2 EXPERIMENTAL PROGRAM

2.1 Specification of Test Specimens

A total of seven full-scale concrete beams reinforced with various bar arrangements of single and bundled GFRP bars were tested under a four-point bending setup to failure. All beams had a clear span of 5000 mm, a shear span of 1250 mm and a constant-moment span of 2500 mm. The gross cross-sectional dimensions of all specimens were 300×450 mm. Figure 1 shows the geometry and transverse reinforcement details of the specimens.

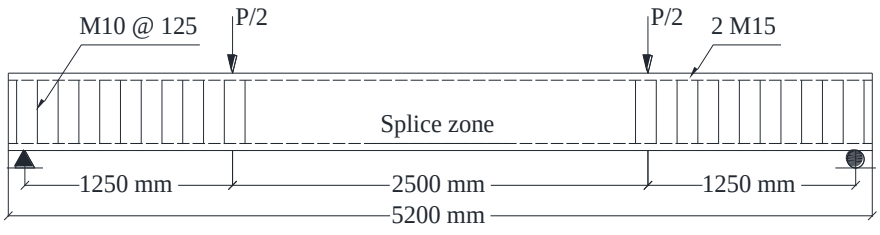

Figure 1: Details of the geometry and transverse reinforcement of the test beams

The shear capacity of specimens was checked as per the recommendations of CSA S806-12 (Canadian Standards Association, 2012), and the shear spans were reinforced with 10M steel stirrups at 125 mm intervals. The side and bottom covers were designed so that the bond splitting failure precedes flexural failure of spliced beams. In this regard, the minimum bottom and side clear covers were, respectively, 32 mm and 45 mm in all beams. Moreover, the clear spacing of the bars was greater than two times the bottom cover, thus, the bond behavior was governed by the bottom cover. In order to evaluate the minimal bound of the splice strength of GFRP bars, no confinement was provided along the splice zone. Nevertheless, the lap splicing of bundled bars with no transverse reinforcement is not in accordance with the design codes(Canadian Standards Association, 2012; ACI Committee 318, 2014). Thus, it is not common in field applications. Two 16 mm steel bars were used as compression reinforcement.

Table 1 lists full details of specimens. In the all splices of bundled bars, a space of 40 mm was left between the ends of two adjacent splices to avoid disruption in the reinforcement surface within splice length due to the installation of strain gages.

Table 1: Details of test beams

Identification	Total Number of Bars	Number of Bars in Bundle	Splice Length	f_c'
			mm	MPa
B4-S100-L320	2	1	320	40.3
B4-D100-L320	4	2	320	39.6
B4-T100-L320	6	3	320	40.9
B4-D-NS	4	2	-	40.3
B4-S50-L320	2	1	320	40.9
B4-D50-L320	4	2	320	40.3
B4-T33-L320	6	3	320	40.9

The identifation code of each specimen starts with the letter B, followed by a number identifying the bar size (4 for No. 4). The second letter indicates the bundle type (S, D, or T for single bars, two-bar bundles, and three-bar bundles, respectively), while the second number (33, 50, or 100) represents the percentage of bars staggered in each section within the splice length. The final digits after the letter L identify the splice length of individual bars in *mm*. Moreover, B4-D-NS is the reference specimens without splice.

2.2 Material Properties

Ribbed steel bars of 16 mm and 11.3 mm diameters were used as compression and transverse reinforcement, respectively. Number 4 (12.7 mm) sand-coated GFRP bars were used as the longitudinal tension reinforcement. Table 2 lists the mechanical properties of the reinforcing bars. The values associated with the GFRP bar were obtained as the average properties of five specimens tested as per CSA S806 (2012), Annex C (Canadian Standards Association, 2012) while those of steel bars are nominal values provided by manufacturer.

Table 2: Mechanical properties of the reinforcing bars

Bar Type	Bar Size	Bar Diameter (mm)	Elastic Modulus (GPa)	Tensile Strength (MPa)	Tensile Strain (%)
GFRP	No.4	12.7	51.7	1243	2.40
Steel	M10	11.3	200	$f_y = 420$	$\varepsilon_y = 0.2$
	M15	16	200	$f_y = 420$	$\varepsilon_y = 0.2$

ε_y = yield strain and f_y = yield stress

The beams were cast using a normal-weight concrete with a target 28-day compressive strength of 35 MPa. The required concrete was delivered by a ready-mix local concrete supplier. Representative 100×200 mm cylinders were cast with the corresponding beams from the same batch of concrete. The beams and

cylinders were stripped one day after casting and then moist-cured for 7 days. They were kept together under ambient conditions until the testing day. Table 1 lists the compressive and splitting tensile strengths obtained by testing five cylinders on the testing day (± 2 days).

2.3 Test Setup and Instrumentation

The specimens were monotonically loaded using a 1000kN hydraulic actuator in a four-point bending setup up to failure. The loading rate was 1.2 mm/min. Figure 2 demonstrates the test setup. As shown, a series of linear variable differential transformers (LVDTs) were used to record displacement variations along the entire span of beams.

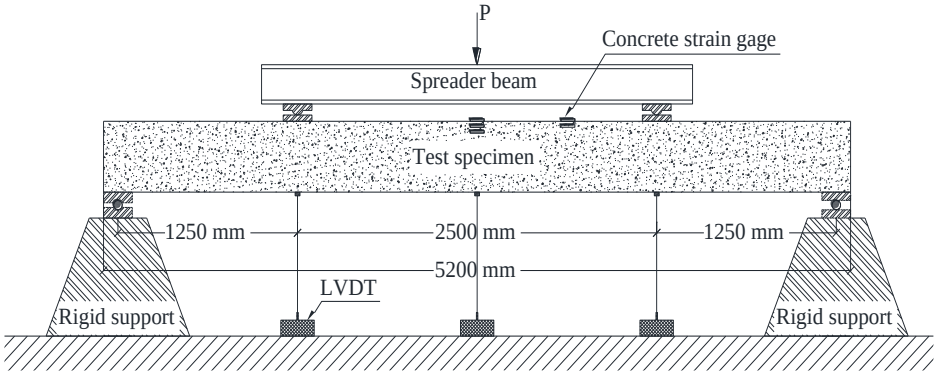

Figure 2: Test setup, and location of LVDTs and concrete strain gages

Loading was paused at the inceptions of the first two cracks which were initiated close to the extremities of splice zone. For each of crack: first, a high precision electronic microscope was used to measure the initial crack width. Then, an LVDT was installed perpendicular to the crack to record the trend of crack width evolution up to failure. The other flexural cracks within the flexural span were visually checked during loading. Due to the safety-related reasons, the visual check was terminated as the applied load approached the expected failure load.

A number of electrical-resistance strain gages were used to record the strain values in the reinforcing bars and concrete as demonstrated in Figure 2. Due to change in beam stiffness at the splice ends, cracks were expected to develop at these locations. Thus, to minimize the possibility of damage caused by cracking, the strain gages were installed 20 mm away from these locations. All experimental data —including load, displacements, crack widths, and strain values— were recorded by an automatic data-acquisition system.

3 TEST RESULTS AND ASSESSMENT OF BOND STRENGTH

The average value of the measured strains in of reinforcing bars was considered as the failure strain of the reinforcement, referred to as ε_{test}. The ε_{test} was then multiplied by the modulus of elasticity (E) of the corresponding bar to calculate the failure stress (f_{test}). The corresponding force at failure was then calculated as $F_{test} = nf_{test}A_b$, where n and A_b are the number of bars and the nominal cross-sectional area of an individual bar within a bundle, respectively.

To exclude the effect of variations in the concrete compressive strength on the calculated bond strengths, albeit negligible, all stresses and forces were normalized by the fourth root of the compressive strengths divided by 40 MPa ($\sqrt[4]{(f_c'/40)}$) as proposed by ACI 408 and other researchers (ACI 408 Committee, 2003; Darwin et al., 2005). Table 3 lists the recorded and normalized experimental results for all the test specimens.

Table 3: Test results

Beam	Recorded			Normalized	
	P_u	ε_{test}	f_{test}	$\varepsilon_{test,n}$	$f_{test,n}$
	kN	με	MPa	με	MPa
B4-S100-L320	50.7	7624	394	7609	393
B4-D100-L320	84.6	6161	319	6176	319
B4-T100-L320	91.6	4610	238	4584	237
B4-D-NS	230.2[+]	-	-	-	-
B4-S50-L320	60.6	8048	416	8003	414
B4-D50-L320	89.8	6575	340	6563	339
B4-T33-L320	134.6	6478	335	6442	333

P_u= maximum applied load; ε_{test}= reinforcement strain at failure; f_{test}= reinforcement stress at failure; $\varepsilon_{test,n}$= normalized reinforcement strain at failure; $f_{test,n}$= reinforcement stress at failure.
[+] the test stopped before failure

4 EFFECTS OF STAGGERING

4.1 Failure Modes

During test, the first flexural crack initiated within the constant-moment span, commonly outside the splice zone. As expected, the first flexural crack within the splice zone normally occurred at the ends of splice. With increasing in applied load, the number and depth of flexural cracks in the constant-moment region increased. At higher load levels, hairline splitting cracks were initiated from the flexural crack in the vicinity of the splice end, and gradually propagated within the splice zone on the tension surface and sides of the beams. The staggered bundled beams failed once an individual pair of spliced bars within the bundle failed. As expected, the failure of spliced beams was the splitting of the concrete cover within the splice zone. In the non-staggered bundled beams (B4-D100-L320 and B4-T100-L320), the failure was sudden and explosive without any sign of hairline cracks on the sides of beams up to failure. Figure 3 shows the failure modes of staggered and non-staggered three-bar bundle beams.

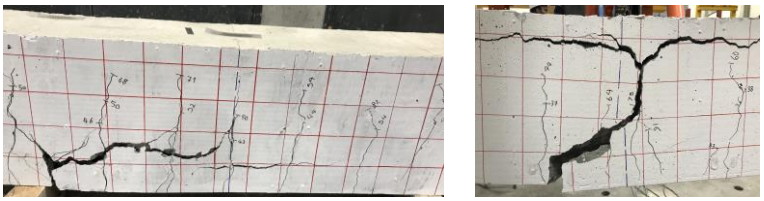

B4-T33-L320 **B4-T100-L320**

Figure 3: Observed failure modes of B4-T33-L320 and B4-T100-L320

4.2 Load–Deflection Behavior

The applied load versus deflection responses of all beams showed a bilinear behavior. There was a substantial reduction in the flexural stiffness after cracking load. In general, all the companion beams, with similar longitudinal reinforcement ratio, displayed similar pre-cracking stiffness. However, the stiffness after cracking was higher for the beams with larger reinforcement ratios. From this observation, it can be concluded that the stiffness after cracking was controlled by the axial stiffness of the longitudinal reinforcement.

Figure 4 shows the load-deflection responses of two-bar bundle specimens. As shown, two-bar bundle beams behaved similarly in terms of pre-cracking stiffness, cracking load and post-cracking stiffness. As shown, both the staggered and non-staggered specimens behaved similar to the reference beam reinforced with continuous bars. Moreover, as can be verified from Table 3 staggering had a minor effect on splice strength of two-bar bundles (319 MPa versus 339 MPa). Therefore, it can be concluded that using two-bar bundled GFRP bars, regardless of staggering pattern, can be a safe practice.

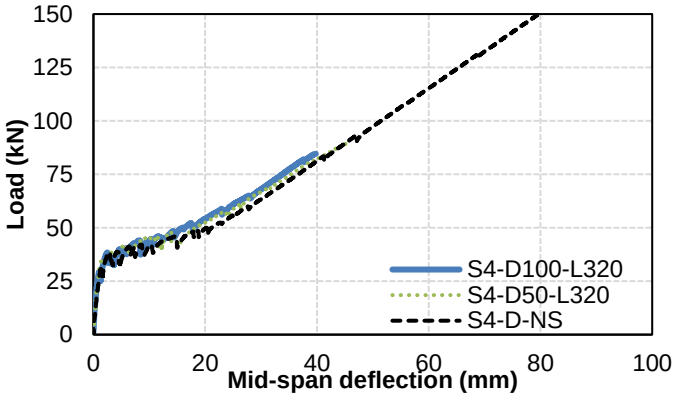

Figure 4: Load-deflection responses of two-bar bundle specimens

All three-bar bundle beams behaved similarly in terms of pre-cracking stiffness, cracking load and post-cracking stiffness. However, the splice strength of the non-staggered specimen was significantly lower than that of staggered specimen (237 MPa versus 333 MPa). Therefore, while the use of staggered three-bar bundle splices can be considered a safe practice, more experimental investigations are required to confirm the feasibility of using non-staggered three-bar bundle splices in practice.

4.3 Crack Width

Visual inspections during test confirmed that, regardless of the staggering pattern, the maximum crack width was normally observed at the splice ends. In other words, the flexural cracks developed in the flexural span outside the splice zone and those within the splice length were narrower than those at the splice ends.

Figure 5 shows the distribution of applied load versus maximum crack width of two-bar bundle specimens. As shown, the non-staggered two-bar bundle specimen (B4-D100-L320) showed wider flexural cracks compared to its companion staggered specimen (B4-D50-L320) and the reference beam (B4-D-NS). Moreover, both specimens reinforced with spliced bars developed wider cracks than the reference specimens. From these observations, it can be concluded that splicing may increase the maximum crack width and that staggering of bundled GFRP bars can help in reducing the maximum crack with.

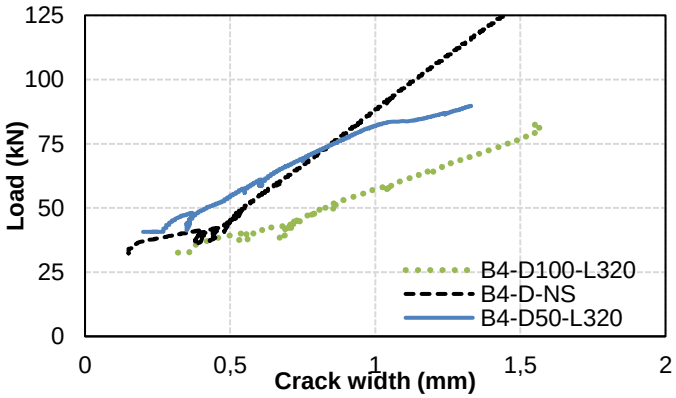

Figure 5: Distribution of applied load versus maximum crack width of two-bar bundle specimens

4.4 Bond strength

The effect of staggering on the behavior of spliced single and bundled bars can be defined by comparing the splice strength and failure load of the companion beams, as listed in Table 4. Overall, staggering could increase the splice strength of bundled bars. However, the improvement in the splice strength was dependent on the number of bars in contact within splice length. The non-staggered single and two-bar bundle splices (B4-S100-L320 and B4-D100-L320) could develop roughly 94% of the strength of their companion staggered beams (B4-S50-L320 and B4-D50-L320, respectively). Nonetheless, staggering had significant effect on the splice strength of three-bar bundles. The normalized splice strength and loading capacity of non-staggered specimen (B4-T100-L320) were 71 and 68% of its staggered counterpart (B4-T33-L320), respectively.

Table 4: Influence of staggering on (a) tensile stress at failure; and (b) failure load

Splice arrangement	$f_{test,n,n\_stg}/f_{test,n,stg}$ †	$P_{u,n,n\_stg}/P_{u,n,stg}$ □
No.4 single	0.95	0.84
No.4 two-bar bundle	0.94	0.94
No.4 three-bar bundle	0.71	0.68

Note:
†: The ratio of normalized bond strength of non-staggered specimen to that of staggered one
□: The ratio of normalized failure load of non-staggered specimen to that of staggered one

5 SUMMARY AND CONCLUSIONS

A total of seven full-scale beam-splice tests were performed to assess the effects of staggering on the bond behavior of spliced bundled GFRP bars in concrete. Based on the experimental findings, the following conclusion remarks can be drawn:

- Regardless of staggering pattern, splicing two-bar bundles is a safe practice.
- Splicing three-bar bundles is a safe practice as long as all bars in a bundle are not spliced at the same section. More experimental investigations are recommended to investigate the feasibility of using non-staggered three-bar bundle splices.
- Staggering had negligible effect on the post-cracking stiffness of the beams. However, it helped in reducing the maximum crack width within flexural span.
- While staggering of reinforcing bars had minor influence on the strength of single and two-bar bundle splices, it could significantly increase the splice strength of the three-bar bundles.

Acknowledgements

This research was conducted with funding from the Tier-1 Canada Research Chair in Advanced Composite Materials for Civil Structures, the Natural Sciences and Engineering Research Council of Canada (NSERC), the NSERC Industrial Research Chair in FRP Reinforcement for Concrete Infrastructure, the Fonds de recherche du Québec en nature et technologies (FRQ-NT), and the Quebec Ministry of Transportation. The authors would like to thank the technical staff of the Canadian Foundation for Innovation (CFI) structural & materials lab in the Department of Civil Engineering at the University of Sherbrooke.

References

ACI 408 Committee. (2003). Bond and Development of Straight Reinforcing Bars in Tension (ACI 408R-03). *American Concrete Institute, Detroit, Michigan, US*.

ACI Committee 318. (2014). Building Code Requirements for Structural Concrete (ACI 318-14) and Commentary (ACI 318R-14). Farmington Hills, Mich.: American Concrete Institute.

ACI Committee 440. (2015). Guide for the Design and Construction of Structural Concrete Reinforced with Fiber-Reinforced Polymer (FRP) Bars (ACI 440.1R-15). Farmington Hills, Michigan, USA: American Concrete Institute.

Aly, R., Benmokrane, B., & Ebead, U. (2006a). Tensile Lap Splicing of Bundled CFRP Reinforcing Bars in Concrete. *Journal of Composites for Construction, 10*(4), 287-294. doi:10.1061/(asce)1090-0268(2006)10:4(287)

Aly, R., Benmokrane, B., & Ebead, U. (2006b). Tensile Lap Splicing of Fiber-Reinforced Polymer Reinforcing Bars in Concrete. *ACI Structural Journal, 103*(6), 857-864. doi:10.14359/18239

Canadian Standards Association. (2012). Design and Construction of Building Structures with Fiber Reinforced Polymers (CAN/CSA S806-12). Ontario, Canada: Canadian Standards Association.

Canadian Standards Association. (2014). Canadian Highway Bridge Design (CAN/CSA S6-14) (pp. 875). Ontario, Canada: CSA Group.

Choi, D.-U., Chun, S.-C., & Ha, S.-S. (2012). Bond strength of glass fibre-reinforced polymer bars in unconfined concrete. *Engineering Structures, 34*(0), 303-313. doi:10.1016/j.engstruct.2011.08.033

Darwin, D., Lutz, L.A., & Zuo, J. (2005). Recommended Provisions and Commentary on Development and Lap Splice Lengths for Deformed Reinforcing Bars in Tension. *ACI Structural Journal, 102*(6), 892-900. doi:10.14359/14798

Esfahani, M.R., Rakhshanimehr, M., & Mousavi, S.R. (2013). Bond Strength of Lap-Spliced GFRP Bars in Concrete Beams. *Journal of Composites for Construction, 17*(3), 314-323. doi:10.1061/(asce)cc.1943-5614.0000359

Harajli, M., & Abouniaj, M. (2010). Bond Performance of GFRP Bars in Tension: Experimental Evaluation and Assessment of ACI 440 Guidelines. *Journal of Composites for Construction, 14*(6), 659-668. doi:10.1061/(asce)cc.1943-5614.0000139

Japan Society of Civil Engineers. (1997). Recommendation for Design and Construction of Concrete Structures Using Continuous Fiber Reinforcing Materials (pp. 1-64).

Mosley, C.P., Tureyen, A.K., & Frosch, R.J. (2008). Bond Strength of Nonmetallic Reinforcing Bars. *ACI Structural Journal, 105*(5), 634-642. doi:10.14359/19947

Pay, A.C., Canbay, E., & Frosch, R.J. (2014). Bond Strength of Spliced Fiber-Reinforced Polymer Reinforcement. *ACI Structural Journal, 111*(2). doi:10.14359/51686519

Tighiouart, B., Benmokrane, B., & Mukhopadhyaya, P. (1999). Bond strength of glass FRP rebar splices in beams under static loading. *Construction and Building Materials, 13*(7), 383-392. doi:10.1016/s0950-0618(99)00037-9

Zemour, N., Asadian, A., Ahmed, E.A., Khayat, K.H., & Benmokrane, B. (2018). Experimental study on the bond behavior of GFRP bars in normal and self-consolidating concrete. *Construction and Building Materials, 189*, 869-881. doi:10.1016/j.conbuildmat.2018.09.045